

1 **Increased air pollution exposure among the Chinese population during the**  
2 **national quarantine in 2020**

3

4 Huizhong Shen<sup>a,b</sup>, Guofeng Shen<sup>b,1</sup>, Yilin Chen<sup>a</sup>, Armistead G. Russell<sup>a</sup>, Yongtao Hu<sup>a</sup>, Xiaoli  
5 Duan<sup>c</sup>, Wenjun Meng<sup>b</sup>, Yang Xu<sup>b</sup>, Xiao Yun<sup>b</sup>, Baolei Lyu<sup>d</sup>, Shunliu Zhao<sup>e</sup>, Amir Hakami<sup>e</sup>, Shu  
6 Tao<sup>b</sup>, Kirk R. Smith<sup>f,1</sup>

7

8 <sup>a</sup>School of Civil & Environmental Engineering, Georgia Institute of Technology, Atlanta, GA  
9 30332, USA

10 <sup>b</sup>College of Urban and Environmental Sciences, Laboratory for Earth Surface Processes, Sino-  
11 French Institute for Earth System Science, Peking University, 100871 Beijing, China

12 <sup>c</sup>School of Energy and Environmental Engineering, University of Science and Technology Beijing,  
13 Beijing 100083, China

14 <sup>d</sup>Huayun Sounding Meteorology Technology Corporation, Beijing, 100081, China

15 <sup>e</sup>Department of Civil and Environmental Engineering, Carleton University, Ottawa, ON K1S 5B6,  
16 Canada

17 <sup>f</sup>Environmental Health Sciences, School of Public Health, University of California, Berkeley, CA  
18 94720-7360, USA

19 <sup>1</sup>To whom correspondence may be addressed. Email: gfshen12@pku.edu.cn;

20 krksmith@berkeley.edu

21

22 **Short title:** The COVID-19 quarantine increased PM<sub>2.5</sub> exposure in China.

23

24

**This is a non-peer reviewed preprint submitted to EarthArXiv.**

25

26

27 **Abstract**

28 The COVID-19 quarantine in China is thought to have been beneficial for reducing the population  
29 exposure to ambient air pollution. The overall exposure also depends, however, on indoor air quality  
30 and human mobility and activities, which also changed during the pandemic. Here we integrate real-  
31 time mobility data, questionnaire survey on during-pandemic human activity patterns, advanced air  
32 quality modeling techniques, and an indoor exposure model. We first show a decrease of  $16.7 \mu\text{g}\cdot\text{m}^{-3}$   
33 <sup>3</sup> in the national average population-weighted ambient  $\text{PM}_{2.5}$  during the quarantine (i.e., the one  
34 month following the start of the Spring Festival holiday). The total population-weighted exposure  
35 (PWE) to  $\text{PM}_{2.5}$  considering both indoor and outdoor environments, however, increased by  $5.7 \mu\text{g}\cdot\text{m}^{-3}$   
36 <sup>3</sup>. The increase in PWE was mainly due to the nationwide population migration from urban to rural  
37 areas before the Spring Festival coupled with the freezing of the migration backward due to the  
38 quarantine ( $+10.8 \mu\text{g}\cdot\text{m}^{-3}$ ), which increased household energy consumption and the fraction of  
39 people exposed to rural household air pollution (HAP) indoors. The changes in PWE due to the  
40 quarantine were  $-14.0$  and  $+19.2 \mu\text{g}\cdot\text{m}^{-3}$  among urban and rural populations, respectively, and ranged  
41 from  $-9.1 \mu\text{g}\cdot\text{m}^{-3}$  in the provinces with the highest per-capita income to  $7.1 \mu\text{g}\cdot\text{m}^{-3}$  in the provinces  
42 with the lowest. HAP contributed 82% of PWE during this period, which was likely more severe  
43 than any period in recent years. Our analysis reveals an increased inequality of air pollution exposure  
44 during the COVID-19 quarantine and highlights the importance of HAP for population health in  
45 China.

46

47

48 **Introduction**

49 Due to the outbreak of COVID-19, China activated the First Level Public Health Emergency  
50 Response (FLPHER, here called a quarantine), which required local governments to carry out strict  
51 restrictions on travel (1, 2). The entire country was under this quarantine, which lasted for one month  
52 and was arguably unprecedented regarding its spatial coverage, duration, strictness, and  
53 effectiveness for preventing the spread of COVID-19 (2). There was an observed improvement in  
54 ambient air quality during the quarantine likely due to the limited industrial and transportation  
55 activities coupled with favorable meteorological conditions (3-8). Some expected that the air quality  
56 improvement may have reduced the exposure of the population to air pollutants, such as NO<sub>2</sub> (6, 7,  
57 9). If coupled with reductions in the ambient levels of fine particulate matter with a diameter smaller  
58 than 2.5 μm (PM<sub>2.5</sub>) for which the best information is available on health impacts, the quarantine  
59 may have yielded an inadvertent health benefit during the COVID-19 pandemic. How actual  
60 population exposure changed, however, depends not only on the ambient air quality but also on the  
61 air quality indoors, and the mobility and daily activity patterns of individuals, such as the time spent  
62 in different locations (10-13).

63

64 The quarantine triggered by the outbreak started from Jan. 25, 2020, which coincided with the start  
65 of the 2020 Spring Festival. Just before the start, reportedly 125 million migrant workers had moved  
66 from urban to rural areas to reunite with their families (14). Normally, they would have returned at  
67 most one month after the start of the Festival (15). Such a nationwide returning-to-work tide,  
68 however, was frozen by travel restrictions under the quarantine (16, 17). Thus, an extra 9% of the  
69 Chinese population were kept in rural areas longer because of the COVID-19 outbreak, where  
70 household air pollution (HAP) is more severe due to the prevalent use of solid fuels (i.e., coal and  
71 biomass) for cooking (13, 18). Also, during that season, there was still significant space heating in  
72 households over much of the country, which is even more likely to be done with solid fuels than  
73 cooking (19).

74

75 The question we ask is how the overall PM<sub>2.5</sub> exposure of the Chinese population changed during

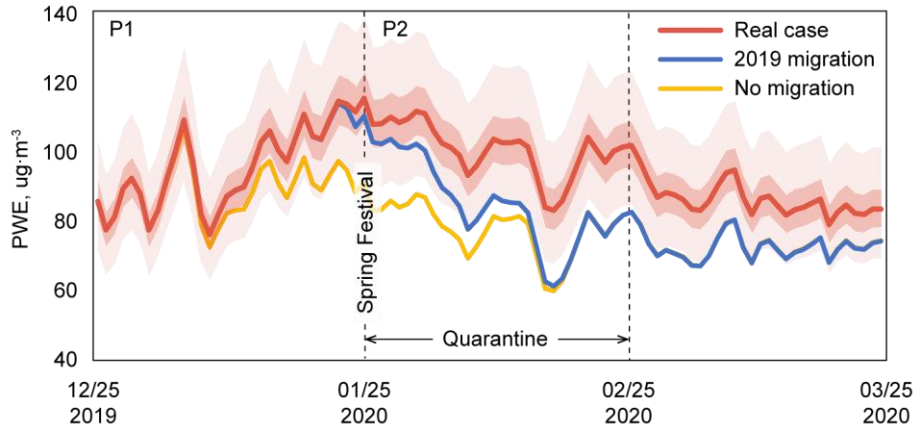
76 the COVID-19 quarantine, taking into account the changes in indoor and outdoor concentrations,  
77 time spent indoors and outdoors, and large-scale migration patterns. Such an assessment is of  
78 interest because of the health impacts of short-term exposure to  $PM_{2.5}$  (20-22) and the reported  
79 associations between  $PM_{2.5}$  and the spread and severity of the COVID-19 infection (23, 24). Here  
80 we use real-time migration data, during-pandemic activity survey data, national census data,  
81 advanced air quality modeling techniques, and an indoor exposure model to track the dynamic  
82 changes in the population exposure to  $PM_{2.5}$  across China before and during the nationwide  
83 quarantine (Materials and Methods).

84

## 85 **Results and Discussion**

86 **Overall change in  $PM_{2.5}$  exposure before and after the COVID-19 quarantine.** We focus our  
87 comparison on two periods—P1, one month preceding the Spring Festival spanning from Dec. 25,  
88 2019 to Jan. 24, 2020, and P2, one month following the start of the Spring Festival, i.e., the  
89 quarantine period, spanning from Jan. 25, 2020 to Feb. 25, 2020 (Figure 1). Using surveys on time-  
90 activity patterns of the Chinese population both in normal days and during the quarantine,  
91 population time use is parsed between indoors and outdoors (Materials and Methods). Data fusion  
92 using an ensemble deep learning method to integrate the ground-level measurements of the national  
93 monitoring network with the outputs of a chemical transport model (25) (Materials and Methods)  
94 shows a decrease of  $16.7 \text{ ug}\cdot\text{m}^{-3}$  ( $15.3\text{--}18.2 \text{ ug}\cdot\text{m}^{-3}$ , uncertainty is expressed as 95% confidence  
95 interval throughout) in the population-weighted average of ambient (outdoor)  $PM_{2.5}$  concentrations  
96 between P1 ( $64, 58\text{--}69 \text{ ug}\cdot\text{m}^{-3}$ ) and P2 ( $47, 43\text{--}51 \text{ ug}\cdot\text{m}^{-3}$ ). In contrast, the population-weighted  
97 exposure (PWE) that considers both indoor and ambient concentrations shows an increase of  $5.7$   
98  $\text{ug}\cdot\text{m}^{-3}$  ( $4.2\text{--}8.2 \text{ ug}\cdot\text{m}^{-3}$ ) in P2 ( $101, 84\text{--}122 \text{ ug}\cdot\text{m}^{-3}$ ) compared to P1 ( $95, 79\text{--}114 \text{ ug}\cdot\text{m}^{-3}$ ) (Figure 1),  
99 suggesting important roles of other factors, including population migration and the time spent  
100 indoors, in the PWE change under the quarantine. Decomposition analysis, by changing the factors  
101 severally, attributes the changes of  $-10.5$  ( $-11.0\text{--}9.3$ ),  $10.8$  ( $7.4\text{--}15.0$ ), and  $5.4$  ( $4.3\text{--}6.9$ )  $\text{ug}\cdot\text{m}^{-3}$  in  
102 PWE to the changes in ambient  $PM_{2.5}$ , population migration, and time spent indoors, respectively  
103 (Figure 2). Note that changes in ambient  $PM_{2.5}$  affect indoor concentration through infiltration,

104 which is included in our assessment. Population migration alone offsets the effect of the ambient air  
105 quality improvement on PWE (10.8 due to migration vs. -10.5  $\mu\text{g}\cdot\text{m}^{-3}$  due to ambient air) (Figure 2).  
106



107

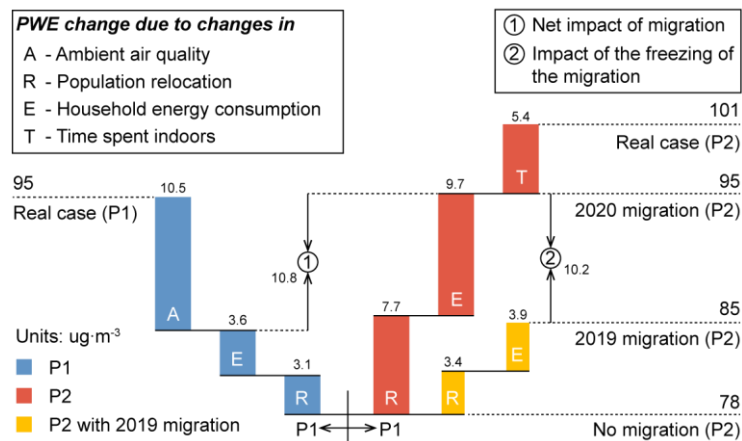
108 **Figure 1. Daily trends of PWE in the real case and under different counterfactual scenarios**  
109 **during the study period.** The dark and light shaded areas represent the inter-quartile range and the  
110 95% confidence interval of the real-case time series, respectively. Compared to the real case, the  
111 “2019 migration” scenario assumes that there was no COVID-19 outbreak such that the migration  
112 followed the pattern of the 2019 Spring Festival (instead of 2020) and the time spent indoors was  
113 not affected by the quarantine. The “no migration” scenario assumes no COVID-19 outbreak and  
114 no Spring Festival migration. Ambient  $\text{PM}_{2.5}$  levels remain the same across the scenarios. The  
115 difference between the real case and the “2019 migration” scenario reflects the impacts of the  
116 quarantine-induced freezing of the migration and the change in time spent indoors on PWE. The  
117 difference between the “2019 migration” and “no migration” scenarios reflects the impact of the  
118 Spring Festival migration on PWE in normal year.

119

120 **The effects of migration on PWE.** The dynamic cross-province migration dataset we established  
121 is based on the national census data (26) and official reports (14) and is temporally allocated using  
122 the Baidu real-time mobility data (27) (Materials and Methods). The direction of the migration is  
123 characterized on a province-to-province basis and further divided into four categories: 1) urban-to-  
124 rural, 2) urban-to-urban, 3) rural-to-rural, 4) rural-to-urban. The migration started about 25 days  
125 before the Spring Festival and had two phases with opposite directions—one occurred in P1, the

126 other in P2. Before the Spring Festival (P1), there were estimated 236 million people returning to  
 127 their hometowns, accounting for one sixth of the total population. Urban-to-rural migration  
 128 contributed 53% of the total, of which the majority were reportedly rural migrant workers (14).  
 129 Urban-to-urban migration contributed 34%, and other two types of migration were relatively minor  
 130 (10% for rural-to-rural, 3% for rural-to-urban). After the Spring Festival (P2) when people would  
 131 normally move back to cities, however, the nation was under quarantine in response to the outbreak  
 132 of COVID-19, and the migration froze. The effect of the quarantine on the migration in P2 is clearly  
 133 illustrated by the day-by-day comparison in the migration intensity in 2020 with the previous year  
 134 (Figure 3). The migration in P2 was close to completion within 25 days after the 2019 Spring  
 135 Festival, by which time this year the migration was only 18% complete (Figure 3).

136



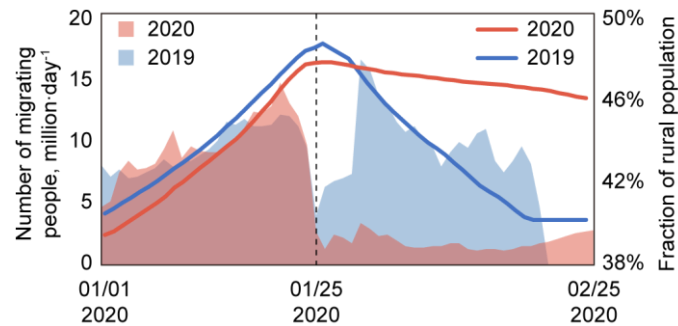
137

138 **Figure 2. Decomposition analysis of the PWE change between P1 and P2.** The overall change  
 139 in the PWE of the Chinese population is decomposed into the changes in PWE due to the changes  
 140 in ambient air quality, population relocation, household energy consumption, and time spent indoors.  
 141 Note that the migration had two phases with opposite directions—the first one (during P1) preceded  
 142 the Spring Festival when people returned to their hometowns, the second (during P2) followed the  
 143 first as people traveled back to work. The quarantine froze the second phase of the migration, leading  
 144 to a net difference in the migration impact on PWEs between P1 and P2, as marked in the figure.  
 145 The impact of the quarantine-induced freezing of the migration in response to COVID-19 in P2 are  
 146 evaluated by comparing with the PWE under 2019 migration pattern and are also marked in the  
 147 figure. PWEs are in  $\mu\text{g}\cdot\text{m}^{-3}$ .

148

149 The migration led to a shift in the fraction of population residing in rural areas. The fraction reached  
150 its maximum of 47.6% during the Spring Festival as did in normal years but decreased at a pace one  
151 seventh the pace of normal years afterwards due to the quarantine (0.05% per day in 2020 vs. 0.34%  
152 per day in 2019) (Figure 3).

153



154

155 **Figure 3. The population migration around the Spring Festivals of 2019 and 2020.** The shaded  
156 areas illustrate the temporal trend of the number of people migrating each day. The solid lines show  
157 the temporal trends of the fraction of rural population (i.e., the population residing in rural areas) in  
158 the total population. The black dashed line marks the Spring Festival. The x-axis represents the  
159 calendar date in 2020.

160

161 Two main consequences of such a change in the migration for population exposure were 1) an larger  
162 fraction of people exposed for a longer time to HAP in rural households which is usually more  
163 severe than in urban households (13, 18) and 2) increased rural energy consumption to meet the  
164 demand of the immigrants, both of which further worsened HAP. Based on a recently conducted  
165 national survey on rural household energy consumption (19) and the indoor exposure model (10, 12)  
166 (Materials and Methods), we estimate that by increasing the fraction of rural population, the  
167 migration enhanced the nationwide PWE by 3.1 and 7.7  $\text{ug}\cdot\text{m}^{-3}$  in P1 and P2, respectively, compared  
168 to a baseline scenario assuming no migration (Figure 2), while by increasing the household energy  
169 consumption, the migration further increased the PWE by 3.6 and 9.7  $\text{ug}\cdot\text{m}^{-3}$ , respectively, in P1  
170 and P2 (Figure 2). This amounts to the total increases of 6.6 and 17.4  $\text{ug}\cdot\text{m}^{-3}$  in PWE in P1 and P2,  
171 respectively. To isolate the impact of the COVID-19-induced freezing of the migration on PWE, we

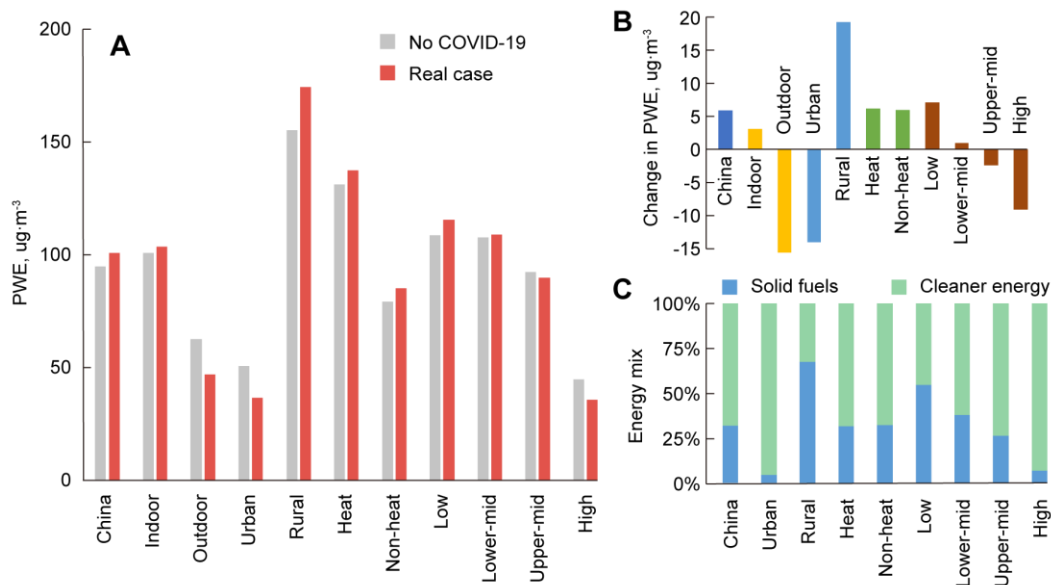
172 substitute 2019's migration for that experienced in 2020 while keeping all other factors equal (i.e.,  
173 outdoor air quality, time spent indoors, baseline energy mix, etc.). The results show a comparable  
174 increase in PWE in P1 ( $6.5 \text{ ug}\cdot\text{m}^{-3}$  in 2019 vs.  $6.6 \text{ ug}\cdot\text{m}^{-3}$  in 2020) but a much smaller increase in  
175 P2 ( $7.2$  vs.  $17.4 \text{ ug}\cdot\text{m}^{-3}$ ), suggesting an enhancement of  $10.2 \text{ ug}\cdot\text{m}^{-3}$  ( $17.4$  minus  $7.2$ ) in PWE due to  
176 the freezing of the migration under the national quarantine.

177

178 **The contribution of HAP on PWE and the inequality of the PWE change.** Focusing on the  
179 quarantine period (P2), we consider the changes in HAP and other sectors (i.e., transportation,  
180 industry, and power generation) and assess the overall impacts of the quarantine on indoor and  
181 ambient air quality and on PWE. Our assessment shows an estimated decrease of  $15.6$  ( $8.6$ – $22.6$ )  
182  $\text{ug}\cdot\text{m}^{-3}$  in the population-weighted average ambient  $\text{PM}_{2.5}$  due to the quarantine, which is similar in  
183 magnitude to the  $\text{PM}_{2.5}$  reduction before and after the COVID-19 outbreak ( $16.7 \text{ ug}\cdot\text{m}^{-3}$ ) (Figure 4).  
184 We note, however, that unlike our fused  $\text{PM}_{2.5}$  field which is the best guess of the real-world  $\text{PM}_{2.5}$   
185 concentrations, our impact assessment on ambient  $\text{PM}_{2.5}$  using chemical transport model is limited  
186 by the uncertainty in the estimation of quarantine-induced emission reduction (Material and  
187 Methods) and the capability of the model to reproduce the actual  $\text{PM}_{2.5}$  change in response to the  
188 emission reduction (28), both of which warrant further investigation. The indoor  $\text{PM}_{2.5}$   
189 concentration is estimated to increase by  $3.1$  ( $2.4$ – $3.8$ )  $\text{ug}\cdot\text{m}^{-3}$  due to the quarantine (Figure 4B)  
190 which is a result of the competition between the exacerbation of HAP ( $12.2 \text{ ug}\cdot\text{m}^{-3}$ ) and the  
191 improvement in ambient  $\text{PM}_{2.5}$  that infiltrates indoors ( $-9.1 \text{ ug}\cdot\text{m}^{-3}$ ). Incorporating the changes in  
192 indoor and ambient  $\text{PM}_{2.5}$  with population migration and human activities, we estimate that the  
193 COVID-19 quarantine led to a net increase of  $5.9$  ( $4.5$ – $7.3$ )  $\text{ug}\cdot\text{m}^{-3}$  in PWE (Figure 4B).

194





195

196 **Figure 4. The impacts of the responses to COVID-19 on PWEs and the use of solid fuels as a**  
 197 **driving factor.** The PWEs in the real case and in the no-COVID-19 scenario (A), the changes in  
 198 PWEs due to the responses to COVID-19 (B), and the shares of solid fuel use in household energy  
 199 mix (C) in China, in indoor/outdoor environments, in urban/rural areas, in heating/non-heating  
 200 regions, and in provinces with different per-capita income levels. The shares of solid fuel use in  
 201 household energy mix in indoor/outdoor environments are the same as in national total, and thus are  
 202 not shown in C.

203

204 We calculate the contribution of HAP on PWE, which includes the direct contributions to indoor  
 205 and outdoor PM<sub>2.5</sub> and the indirect contribution of outdoor HAP to indoor PM<sub>2.5</sub> through infiltration  
 206 (Figure S1). HAP dominated the PWE in P2 regardless of whether there was a quarantine, whereas  
 207 the COVID-19-induced quarantine increased the HAP contribution on PWE from 74% (no  
 208 quarantine or no COVID-19) to 82% (in the real case) (Figure S2).

209

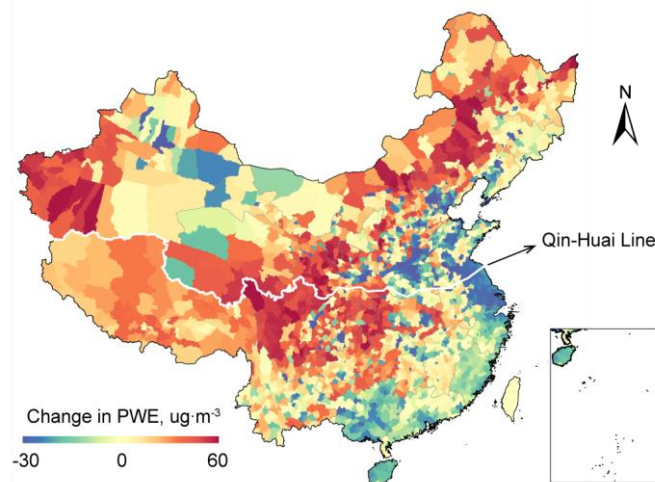
210 The contribution of HAP to PWE during this period was higher than that before the COVID-19  
 211 quarantine (68%), or in a counterfactual scenario where there was no migration (70%), or for annual  
 212 average (62%) (Figure S2). The leading cause of HAP is the use of solid fuels (e.g., coals and  
 213 biomass) for cooking and heating, which is much more prevalent in rural areas (67.5% as the share  
 214 of solid fuels in the household energy mix) than in urban areas (4.7%) (Figure 4C). Further

215 investigation shows a clear tendency toward a stronger positive effect of the quarantine on PWE as  
216 the share of solid fuel use increased (Figure 4B and C and Figure S3) and that the PWE in rural  
217 areas was estimated to increase by  $19.2 \text{ ug}\cdot\text{m}^{-3}$  due to the quarantine, while the urban PWE decreased  
218 by  $14.0 \text{ ug}\cdot\text{m}^{-3}$ .

219

220 The change in exposure associated with solid fuel use and the contrary changes in rural and urban  
221 PWEs are due primarily to the interaction between HAP and the human activities: the longer time  
222 spent indoors during the pandemic increased the time length for people being exposed to HAP and  
223 thus increased the PWE among rural residents; the freezing of the migration in the meanwhile  
224 increased the rural household energy consumption and subsequently increased the severity of HAP.  
225 On the other hand, in urban areas where indoor air quality is often better than outdoor (29), the  
226 increase in the time spent indoors reduced PWE.

227



228

229 **Figure 5. The spatial distribution of the changes in PWE among the Chinese population due**  
230 **to responses to COVID-19. Changes in ambient and indoor air quality, population migration,**  
231 **and time spent indoors are considered.** The PWE changes are illustrated by county. The white  
232 line marks China's Qinling Mountains-Huai River Line (Qin-Huai Line) Qin-Huai Line divides  
233 China into two regions that differ in climate and is commonly used as a reference line in policy  
234 making to determine the heating (northern) and non-heating (southern) regions (30).

235

236 The association between PWE and HAP led to the spatial heterogeneity (Figure 5) and population  
237 inequality in the quarantine-induced changes in PWE (Figure 4C) which ranged from  $-19.0 \text{ ug}\cdot\text{m}^{-3}$   
238  $^3$  in Tianjin to  $32.5 \text{ ug}\cdot\text{m}^{-3}$  in Inner Mongolia and from  $-9.5 \text{ ug}\cdot\text{m}^{-3}$  in the provinces with average  
239 per-capita incomes higher than 5000 USD to  $6.5 \text{ ug}\cdot\text{m}^{-3}$  in the provinces with average per-capita  
240 incomes lower than 3000 USD, suggesting unequal changes in PWE by income group. The  
241 inequality in the PWE changes is further confirmed by the significant negative correlation between  
242 the PWE changes and provincial per-capita income levels ( $p = 2 \times 10^{-4}$ ) and survives the assessments  
243 using county-level data or focusing on the rural population exclusively (Figure S4A and B).

244

245 The urban population does not show significant inequality (Figure S4C) likely due to the much less  
246 dependence on solid fuels and therefore being less affected by HAP than their rural counterparts.  
247 Regression analysis reveals a significant interaction between the per-capita income and the epidemic  
248 severity in the model to predict the quarantine-induced changes in PWE and suggests that regions  
249 with more severe epidemic situation are associated with greater inequality. In Hubei, every 20%  
250 reduction in income is estimated to be associated with a  $6.7 \text{ ug}\cdot\text{m}^{-3}$  increase in PWE due to the  
251 quarantine, which is almost twice the increase ( $3.4 \text{ ug}\cdot\text{m}^{-3}$ ) for the national average (Figure S4A).

252

253 **The effect of Clean Heating Plan on the PWE changes.** Despite the heterogeneity and inequality,  
254 the quarantine-induced increases in PWE in the heating (north) and non-heating (south) regions are  
255 found to be comparable ( $6.2$  and  $5.9 \text{ ug}\cdot\text{m}^{-3}$  in heating and non-heating regions, respectively) (Figure  
256 4B and Figure 5). We find that a recently implemented campaign called “Clean Winter Heating Plan  
257 in Northern China” (“Clean Heating Plan” for short), played an important role in balancing the PWE  
258 increases between heating and non-heating regions. Clean Heating Plan was launched by the  
259 Chinese central government in 2017 and set stringent and differentiate goals through 2021 toward  
260 a high rate of clean heating (i.e., the rate of clean energy used for heating) in the northern region,  
261 with the rates ranging from 40% in rural areas to 100% in some major cities (31). This campaign, if  
262 successfully implemented, would reduce the amount of annual coal consumption by 150 Tg, and  
263 recent progress has shown much success in the implementation of this campaign such that it is

264 expected to be achieved ahead of schedule (32).

265

266 We estimate that Clean Heating Plan had phased out 44.4% of the solid fuels used in households in  
267 the Northern provinces by the end of 2019. If there was no such a campaign, we estimate that the  
268 COVID-19-induced increase in PWE would be almost doubled in the heating region ( $12.0 \text{ ug}\cdot\text{m}^{-3}$ ).  
269 In addition, the population inequality in the PWE increase, measured by the increase in PWE per  
270 20% reduction in income, would be 30.1% higher than is estimated in the real case ( $4.6 \text{ vs. } 3.5 \text{ ug}\cdot\text{m}^{-3}$ )  
271 <sup>3</sup>) in the heating region (Materials and Methods). In an ideal case where Clean Heating Plan was  
272 fully phased in, the quarantine would only lead to an increase of  $2.3 \text{ ug}\cdot\text{m}^{-3}$  in PWE in the heating  
273 region, with the inequality decreased by 15.6%. Our analysis thus reveals that Clean Heating Plan  
274 moderated the quarantine-induced increases in PWE in the heating region, reduced the inequality of  
275 the PWE increases among different income groups of people, and put the PWE increases of the  
276 heating and non-heating regions in the balance. Still, the PWE in the heating region ( $137 \text{ ug}\cdot\text{m}^{-3}$ )  
277 was 61% higher than was in the non-heating region ( $85 \text{ ug}\cdot\text{m}^{-3}$ ), and the quarantine-induced increase  
278 in rural PWE in the heating region ( $24.4 \text{ ug}\cdot\text{m}^{-3}$ ) was 31% higher than was in the non-heating region  
279 ( $18.6 \text{ ug}\cdot\text{m}^{-3}$ ).

280

281 **Conclusion.** In this study, we integrate multiple data sources and modeling techniques to  
282 dynamically track the changes in PWE due to the national quarantine. We first show that the national  
283 population-weighted exposure to ambient  $\text{PM}_{2.5}$  reduced by  $16.7 \text{ ug}\cdot\text{m}^{-3}$ . This is approximately a 26%  
284 drop compared to the 40–60% drop reported widely (4, 8, 33, 34) for ambient  $\text{NO}_2$  levels (not  
285 populations-weighted) measured by ground-level monitors and satellites. This difference is  
286 apparently due to the different emission source characteristics of the two pollutants, with  $\text{NO}_2$   
287 coming mainly from vehicles and industry (35), which were substantially curtailed during the  
288 quarantine (28). A much greater proportion of  $\text{PM}_{2.5}$ , on the other hand (36), comes from household  
289 fuels use of which probably grew during the quarantine.

290

291 We show that, the average PWE of the population is estimated to increase despite a decrease in

292 ambient PM<sub>2.5</sub>, which is mainly due to the worsened HAP and a higher opportunity for people to be  
293 exposed to HAP during the pandemic. Changes to the actual dose of PM<sub>2.5</sub> to the population of  
294 course, will also depend on changes in use and effectiveness of facemasks during the period.

295

296 With respect to the distribution of PWE, our assessment reveals an increase in the environmental  
297 inequality of air pollution exposure in response to the COVID-19 crisis. While the high-income  
298 group benefited from the reduction of PWE, the low-income group suffered a significant increase  
299 in PWE. Such inequality would be even higher if Clean Heating Plan that targets HAP in the  
300 northern China was not implemented. In addition, given the reported association between short-term  
301 exposure to air pollution and the transmission of COVID-19 (23), this analysis shows how the  
302 COVID-19 pandemic itself as well as the quarantine may have deepened health inequalities. Our  
303 assessment highlights the importance of mitigating HAP for reducing the environmental inequality  
304 and protecting human health. If society is to confine people to their homes for their protection, it is  
305 far better that they are clean to start with.

306

## 307 **Methods and Materials**

### 308 **Household energy consumption**

309 Provincial-level household energy consumption data were collected and compiled based on a  
310 representative national survey (19) and China Statistical Yearbook (43). The data were downscaled  
311 to county level and extrapolated to 2020 (the study year) based on the fuel-type-specific empirical  
312 models developed by Shen et al. (38). Following a previous study (10), the clean heating targets set  
313 by Clean Heating Plan were incorporated into the energy trends in the heating region.

### 314 **Migration data**

315 We derived detailed origin and destination information from the 6<sup>th</sup> National Census (26) to  
316 characterize population migration on the county level (38). The census data classified the migrants  
317 into four groups—rural-to-urban, urban-to-urban, rural-to-rural, and urban-to-rural, and are  
318 representative of the migration pattern in 2010. The census data showed a total of 138 million  
319 migrant workers in 2010, noting that not all the migrants intended to return home during the Spring

320 Festival holidays. The Ministry of Human Resources and Social Security reported 125 million  
321 migrant workers returning home in 2020 (14). Therefore, the census data was scaled down by a  
322 factor of 0.9 to represent the migration pattern in 2020. We assumed that all the back-home  
323 migrations were achieved before the second day of the Spring Festival holidays, and that the  
324 returning-to-work migration started from the first day of the Spring Festival holidays. The migration  
325 flows (i.e., the number of migrants) were temporally allocated using the daily cross-province  
326 mobility intensities reported by the Baidu real-time mobility monitoring platform as a surrogate (27).  
327 For the 2019 Spring Festival of which the detailed provincial-level Baidu mobility data were not  
328 available, the national-level mobility intensities were used to scale the 2020 migration pattern to  
329 2019, assuming that the relative difference in the migration flows across provinces remained  
330 unchanged between 2019 and 2020.

### 331 **Survey on human activity pattern**

332 The information on the daily time spent indoors and in different indoor compartments (i.e., kitchen,  
333 living room, and bedroom) in wintertime were derived from Exposure Factors Handbook of Chinese  
334 Population (39), as summarized by Chen et al. (12), and were used in this study to represent the  
335 time-activity pattern when there was no COVID-19. The time-activity pattern during the pandemic  
336 were derived from an online questionnaire survey (<https://www.wjx.cn/m/59666734.aspx>) which  
337 collected information on the frequencies of going out during the quarantine. This survey adopted  
338 strict quality control measures during data processing and analysis. The questionnaires with missing  
339 values, logical errors and data format errors were excluded. Two groups of personnel independently  
340 derived the data and completed the comparison to ensure the accuracy of the results. 8330  
341 questionnaires were distributed with a recovery rate of 100%. A total of 7784 valid questionnaires  
342 were obtained, covering 31 provinces in China. The survey showed that the more severe the  
343 epidemic, the less frequently people went out each day. The frequency data were translated into the  
344 time length of outdoor stay by assuming time lengths for each going-out event ranging from 200  
345 minutes per time in the provinces that were the least affected by the COVID-19 outbreak (i.e.,  
346 Qinghai and Tibet) to 120 minutes per time in Hubei where the outbreak was the most severe. The  
347 uncertainty induced by this assumption was considered in the uncertainty analysis specified in  
348 following section. The average time spent indoors by province before and during the pandemic was

349 summarized in Table S1.

### 350 **Emissions and air quality modeling**

351 We used AiMa emission inventory (41, 42) as the emission input to conduct the air quality modeling  
352 for ambient PM<sub>2.5</sub> assessment. The emission inventory has been compiled by integrating a variety  
353 of inventories and activity data (42) and has undergone continuous updates. This inventory is  
354 currently used by an online operational system (called “AiMa” system) that provides air quality  
355 forecast for government and public (<http://www.aimayubao.com/>). The base year of the latest  
356 version of AiMa inventory is 2017.

357 The ambient PM<sub>2.5</sub> concentrations were obtained by combining hourly ground-level observations  
358 reported by the China National Urban Air Quality Real-time Publishing Platform (5) with model  
359 predictions by the Community Multiscale Air Quality (CMAQ) model (44) using an ensemble deep  
360 learning data fusion approach (25). Meteorological variables were derived from the AiMa system,  
361 which were generated by the Weather Research Forecasting (WRF) model version 3.4.1 (45) driven  
362 by the 0.5-degree global weather forecast products produced by the National Centers for  
363 Environmental Prediction Global Forecast System (46). The downscaled meteorology together with  
364 the AiMa emission inventory was used to drive CMAQ simulation which was conducted to cover  
365 the mainland China on a horizontal resolution of 12 km with 13 vertical layers extending up to ~16  
366 km above ground. The model output was fused with observations to get the final ambient PM<sub>2.5</sub>  
367 concentration fields across China on a daily resolution over the study period (i.e., from Dec. 25,  
368 2019 to Mar. 25, 2020). More details about the emission inventory, the model configuration, the  
369 data fusion approach and its performance can be found in a previous study (25).

370 We conducted adjoint analysis to decompose the contributions of various emission sources to  
371 outdoor PM<sub>2.5</sub> concentrations. The emission sources, as categorized in the AiMa inventory, included  
372 power generation, industry, residential (i.e., household), transportation, agriculture, solvent usage,  
373 fugitive dust, and fires. CMAQ-Adjoint version 5.0 (40) was applied to calculate the adjoint  
374 sensitivities. The adjoint analysis provides location- and time-specific gradients (i.e., adjoint  
375 sensitivities) and can be used in applications such as backward sensitivity analysis, source  
376 attribution, optimal pollution control, data assimilation and inverse modeling (40). The CMAQ-

377 Adjoint version 5.0 is the most up-to-date version of CMAQ-Adjoint. Discrete adjoint is  
378 implemented for gas-phase chemistry, aerosol formation, cloud chemistry and dynamics, and  
379 diffusion. Continuous adjoint is implemented for advection. The model performance has been  
380 comprehensively evaluated in the previous study (40), showing good agreements with the results  
381 given by forward sensitivity analysis.

382 In this study, the cost function of the adjoint analysis was defined as the ambient population  
383 weighted average PM<sub>2.5</sub> concentration over the study period across China. The adjoint model thus  
384 provided sensitivities of this cost function to per-unit emissions of various species in each model  
385 grid cell. Using the source-specific emission information, we evaluated the source contributions of  
386 household (i.e., residential) energy consumption and other sectors on ambient air pollution by  
387 province. Details about the principle equations, development, and evaluation of CMAQ-Adjoint can  
388 be found in previous studies (40, 47).

389 Using the adjoint sensitivities, we further evaluated the changes in the population-weighted  
390 concentration in response to the emission reduction during the quarantine. Following previous study  
391 (28), we assumed a reduction of 10% in power plant emissions, 30% in industrial emissions, and  
392 70% in mobile emissions. The changes in residential emissions due to population migration were  
393 evaluated using the procedures as specified in our previous studies (37, 38).

#### 394 **Indoor exposure model**

395 We employed an indoor exposure model developed by Chen et al. (12) to quantify the indoor PM<sub>2.5</sub>  
396 levels. The model was modified to take into account the change in the amount of household energy  
397 consumption and outdoor infiltration and to unify the estimation approach for urban and rural  
398 household conditions as follows,

$$399 \quad C_{in} = C_{in,add} + C_{out,add} \quad (1)$$

400 where  $C_{in}$  is the indoor PM<sub>2.5</sub> concentration in  $\mu\text{g}\cdot\text{m}^{-3}$ ,  $C_{in,add}$  is the  $C_{in}$  component contributed by  
401 indoor sources, and  $C_{out,add}$  is the  $C_{in}$  component contributed by outdoor infiltration.  $C_{in,add}$  was  
402 calculated by the following equation,

$$403 \quad C_{in,add} = \frac{\sum E_f \cdot C_{f,k} \cdot T_k}{E \cdot \sum T_k} \quad (2)$$



404 where subscripts  $f$  and  $k$  denote the type of fuel (i.e., wood, straw, coal, and cleaner energy) and  
405 indoor compartment (i.e., kitchen, living room, and bedroom), respectively;  $E_f$  is the per-household  
406 daily consumption of fuel type  $f$  in terms of thermal energy amount (i.e., the amount of energy  
407 consumption after thermal efficiency conversion);  $\bar{E}$  is the average per-household daily thermal  
408 energy required for cooking and heating;  $C_{f,k}$  is the  $C_{in,add}$  in indoor compartment  $k$  when  $E_f = \bar{E}$  and  
409 the household consumes fuel  $f$  solely;  $T_k$  is the time spent daily in indoor compartment  $k$ . Following  
410 a previous study (48), the thermal efficiencies of biomass, coal, gas, and electricity are 0.154, 0.244,  
411 0.555, and 0.84, respectively.  $\bar{E}$  values  $40 \text{ MJ}\cdot\text{day}^{-1}\cdot\text{household}^{-1}$  which was calculated as the national  
412 average daily household thermal energy consumption for cooking and heating in winter.  $C_{f,k}$  values  
413 were adopted from a previous study (12) in which the means and variations of  $C_{f,k}$  were determined  
414 by meta-analysis through literature review. The mean heating-season  $C_{f,k}$  in kitchen/living room are  
415 283, 434, and  $547 \mu\text{g}\cdot\text{m}^{-3}$  for coal, crop, and wood, respectively, and in bedroom are 211, 267, 359  
416  $\mu\text{g}\cdot\text{m}^{-3}$  for coal, crop, and wood, respectively. Cleaner energy was assumed to cause little addition  
417 to indoor  $\text{PM}_{2.5}$ , and thus the  $C_{f,k}$  for cleaner energy was set to be 0. Equation (2) assumes that with  
418 all others equal,  $C_{in,add}$  is proportional to the thermal amount of daily energy consumption of the  
419 household. This assumption was testified and supported by sensitivity tests using a single-box model  
420 (49), as recommended in World Health Organization's indoor air quality guidelines (50), to predict  
421  $C_{in,add}$  based on varying amounts of energy consumption.  $C_{out,add}$  was calculated by multiplying  
422 ambient  $\text{PM}_{2.5}$  concentrations with region-specific infiltration factors following Xiang et al.'s  
423 method (51). The  $\text{PM}_{2.5}$  exposure of individuals at a specific location was calculated as the average  
424 of the indoor and outdoor  $\text{PM}_{2.5}$  concentrations weighted by the time fractions of indoor and outdoor  
425 stays. The PWE in a region was calculated as the population-weighted average of the individuals'  
426 exposure within this region. The same approach to calculate PWE has been adopted in previous  
427 studies (10, 11).

#### 428 **Regression analysis**

429 We conducted regression analysis to predict the county-level quarantine-induced changes in PWE.  
430 The regression showed significant interaction between per-capita income and the epidemic severity.  
431 The regression equation is as follows,

$$432 \quad dPWE = -31.9 \times \ln(INC_{per}) - 0.69 \times SEV \times \ln(INC_{per}) + 124.6 \quad (3)$$

433 where  $dPWE$  denotes the change in PWE due to the COVID-19 induced quarantine, in  $\mu\text{g}\cdot\text{m}^{-3}$ ;  
 434  $INC_{per}$  is per-capita annual income, in USD;  $SEV$  is the epidemic severity determined by the  
 435 confirmed cases in the provinces (Table S1), ranging from 1 in Qinghai and Tibet (the least severe)  
 436 to 5 in Hubei (the most severe).

#### 437 **Uncertainty analysis**

438 The uncertainty in the PWE estimates stemmed from various sources, including the uncertainties in  
 439 the modeled ambient and indoor concentrations, population migration, and time-activity patterns.  
 440 We conducted Monte Carlo simulation to propagate the uncertainties from the input variables to  
 441 PWE. For most input variables (e.g., concentration, migration intensity, time spent indoors, etc.),  
 442 we assumed log-normal distributions to avoid negative values and used geometric coefficient of  
 443 variation (GCV) (52) to measure the uncertainty. GCV is defined as follows,

$$444 \quad GCV = e^\sigma - 1 \quad (4)$$

445 where  $e^\sigma$  is the geometric standard deviation (53). According to the performance of the data fusion  
 446 approach evaluated in a previous study which showed good agreement with an independent  
 447 observation dataset (25), the GCV of the population-weighted average of the fused  $\text{PM}_{2.5}$   
 448 concentrations was derived as 4.4%. Given the large uncertainty in the estimated emission reduction  
 449 due to the responses to COVID-19, the GCV for the emission reduction was set to be 40%. The  
 450 GCVs of the population migration intensity and the time spent indoors during the quarantine were  
 451 assumed to be 20% and 10%, respectively. For the time spent indoors in normal days, GCV of 5%  
 452 was used based on the method of Chen et al. (12). For  $\bar{E}$ , we assumed a uniform distribution with a  
 453 variation interval of 20% which is usually applied to reflect the uncertainty in the statistics of  
 454 household solid use (37, 54). The CVs of the infiltration factors in indoor/outdoor air exchange was  
 455 set to be 12.5% following Shi et al. (55). The uncertainties in indoor  $\text{PM}_{2.5}$  concentrations in  
 456 households using solid fuels were derived by Chen et al. based on 1821 observations collected from  
 457 the literature (12). Monte Carlo simulations were performed 1,000,000 times to propagate the  
 458 uncertainties in these input variables into the uncertainty in PWE.

#### 459 **Data availability**

460 The population distribution data, the daily cross-province migration data, the daily ground-level  
461 PM<sub>2.5</sub> fusion data, and all data used to generate the figures in the main text are openly available on  
462 Open Science Framework at <https://osf.io/x46tb/>.

#### 463 **Code availability**

464 The CMAQ source code can be accessed at <https://www.epa.gov/cmaq/how-cite-cmaq>. Upon  
465 completion of expanded user testing, the CMAQ Adjoint code will be hosted and distributed by U.S.  
466 EPA.

467

468 **Acknowledgements.** We thank Haoran Xu, Wenxiao Zhang, Xinyuan Yu, Yu'ang Ren, and Weiying  
469 Hou for their help with the energy data collection and the indoor model development. This work is  
470 funded by the Chinese Academy of Science (XDA23010100), the National Natural Science  
471 Foundation of China (Grant 41830641, 41629101, 41991312, 41922057, and 41821005), the U.S.  
472 Environmental Protection Agency (EPA grant number R835880), and the National Science  
473 Foundation (NSF SRN grant number 1444745). Its contents are solely the responsibility of the  
474 grantee and do not necessarily represent the official views of the supporting agencies. Further, the  
475 US government does not endorse the purchase of any commercial products or services mentioned  
476 in the publication.

477

#### 478 **References**

- 479 1. Xinhua News (2020) 30 provinces activated First-level Public Health Emergency Response,  
480 [http://www.xinhuanet.com/politics/2020-01/25/c\\_1125502232.htm](http://www.xinhuanet.com/politics/2020-01/25/c_1125502232.htm).
- 481 2. Tian H, *et al.* (2020) An investigation of transmission control measures during the first 50  
482 days of the COVID-19 epidemic in China. *Science* 368(6491):638-642.
- 483 3. CNN News (2020) There's an unlikely beneficiary of coronavirus: The planet,  
484 <https://edition.cnn.com/2020/03/16/asia/china-pollution-coronavirus-hnk-intl/index.html>.
- 485 4. Bauwens M, *et al.* (2020) Impact of coronavirus outbreak on NO<sub>2</sub> pollution assessed using  
486 TROPOMI and OMI observations. *Geophys. Res. Lett.*:e2020GL087978.
- 487 5. China National Environmental Monitoring Center (2020) China National Urban Air Quality  
488 Real-Time Publishing Platform. <http://www.cnemc.cn/>.
- 489 6. He G, Pan Y, & Tanaka T (2020) COVID-19, City Lockdowns, and Air Pollution: Evidence  
490 from China. *medRxiv*. doi: <https://doi.org/10.1101/2020.03.29.20046649>.
- 491 7. Venter ZS, Aunan K, Chowdhury S, & Lelieveld J (2020) COVID-19 lockdowns cause global  
492 air pollution declines with implications for public health risk. *medRxiv*. doi:

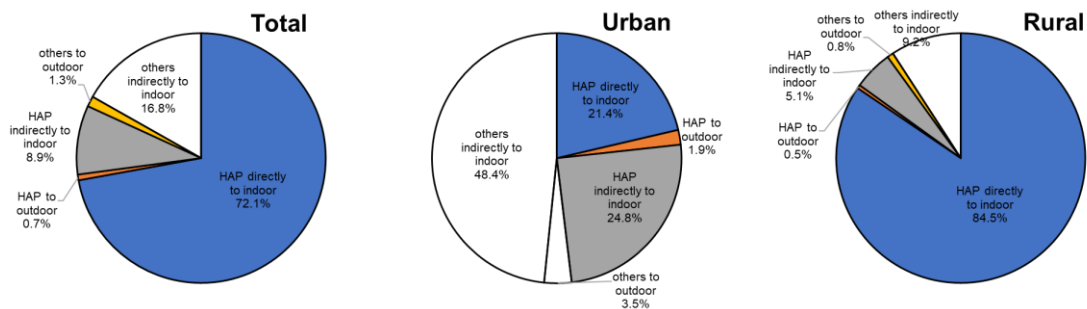
- 493 <https://doi.org/10.1101/2020.04.10.20060673>
- 494 8. Zhao Y, *et al.* (2020) Substantial Changes in Nitrogen Dioxide and Ozone after Excluding  
495 Meteorological Impacts during the COVID-19 Outbreak in Mainland China. *Environmental*  
496 *Science & Technology Letters* <https://doi.org/10.1021/acs.estlett.0c00304>.
- 497 9. Isaifan R (2020) The dramatic impact of Coronavirus outbreak on air quality: Has it saved as  
498 much as it has killed so far? *Global Journal of Environmental Science and Management*  
499 6(3):275-288.
- 500 10. Meng WJ, *et al.* (2019) Energy and air pollution benefits of household fuel policies in  
501 northern China. *Proc. Natl. Acad. Sci. U. S. A.* 116(34):16773-16780.
- 502 11. Zhao B, *et al.* (2018) Change in household fuels dominates the decrease in PM<sub>2.5</sub> exposure  
503 and premature mortality in China in 2005–2015. *Proceedings of the National Academy of*  
504 *Sciences* 115(49):12401-12406.
- 505 12. Chen YL, *et al.* (2018) Estimating household air pollution exposures and health impacts from  
506 space heating in rural China. *Environ. Int.* 119:117-124.
- 507 13. Smith KR, *et al.* (2014) Millions dead: how do we know and what does it mean? Methods  
508 used in the comparative risk assessment of household air pollution. *Annu. Rev. Public Health*  
509 35:185-206.
- 510 14. Central People's Government of the People's Republic of China (2020) *A press conference*  
511 *held by the Ministry of Human Resources and Social Security to introduce the progress of the*  
512 *human and social departments' work related to the epidemic.* [http://www.gov.cn/xinwen/2020-](http://www.gov.cn/xinwen/2020-03/19/content_5493239.htm)  
513 [03/19/content\\_5493239.htm](http://www.gov.cn/xinwen/2020-03/19/content_5493239.htm)
- 514 15. Ministry of Transport of the People's Republic of China (2020) *Big data: the travel volume*  
515 *predictions during Lunar New Year holiday in 2020.*  
516 [http://www.mot.gov.cn/fenixigongbao/yunlifexi/202001/t20200109\\_3322161.html](http://www.mot.gov.cn/fenixigongbao/yunlifexi/202001/t20200109_3322161.html)
- 517 16. Kraemer MU, *et al.* (2020) The effect of human mobility and control measures on the  
518 COVID-19 epidemic in China. *Science* 368(6490):493-497.
- 519 17. Xinhua News (2020) Traffic system works well in the seventh day of the Spring Festival  
520 holiday, [http://www.xinhuanet.com/politics/2020-01/30/c\\_1125514185.htm](http://www.xinhuanet.com/politics/2020-01/30/c_1125514185.htm).
- 521 18. Zhang JJ & Smith KR (2007) Household air pollution from coal and biomass fuels in China:  
522 Measurements, health impacts, and interventions. *Environ. Health Perspect.* 115(6):848-855.
- 523 19. Tao S, *et al.* (2018) Quantifying the rural residential energy transition in China from 1992 to  
524 2012 through a representative national survey. *Nature Energy* 3(7):567-573.
- 525 20. Di Q, *et al.* (2017) Association of short-term exposure to air pollution with mortality in older  
526 adults. *JAMA* 318(24):2446-2456.
- 527 21. Dominici F, *et al.* (2006) Fine particulate air pollution and hospital admission for  
528 cardiovascular and respiratory diseases. *JAMA* 295(10):1127-1134.
- 529 22. Katsouyanni K, *et al.* (1997) Short term effects of ambient sulphur dioxide and particulate  
530 matter on mortality in 12 European cities: results from time series data from the APHEA  
531 project. *BMJ* 314(7095):1658.
- 532 23. Yongjian Z, Jingu X, Fengming H, & Liqing C (2020) Association between short-term  
533 exposure to air pollution and COVID-19 infection: Evidence from China. *Sci. Total*  
534 *Environ.*:138704. doi: 10.1016/j.scitotenv.2020.138704.
- 535 24. Wu X, Nethery RC, Sabath BM, Braun D, & Dominici F (2020) Exposure to air pollution and  
536 COVID-19 mortality in the United States. *medRxiv*. doi:

- 537 <https://doi.org/10.1101/2020.04.05.20054502>.
- 538 25. Lyu B, *et al.* (2019) Fusion Method Combining Ground-Level Observations with Chemical  
539 Transport Model Predictions Using an Ensemble Deep Learning Framework: Application in  
540 China to Estimate Spatiotemporally-Resolved PM<sub>2.5</sub> Exposure Fields in 2014–2017.  
541 *Environ. Sci. Technol.* 53(13):7306-7315.
- 542 26. National Bureau of Statistics of the People's Republic of China (2011) Census Data.  
543 <http://www.stats.gov.cn/tjsj/pcsj/>.
- 544 27. Baidu Inc (2020) Baidu migration, <https://qianxi.baidu.com/2020/>.
- 545 28. Huang X, *et al.* (2020) Enhanced secondary pollution offset reduction of primary emissions  
546 during COVID-19 lockdown in China. doi: 10.31223/osf.io/hvuzy
- 547 29. Qi M, *et al.* (2017) Exposure and health impact evaluation based on simultaneous  
548 measurement of indoor and ambient PM<sub>2.5</sub> in Haidian, Beijing. *Environ. Pollut.* 220:704-712.
- 549 30. Chen Y, Ebenstein A, Greenstone M, & Li H (2013) Evidence on the impact of sustained  
550 exposure to air pollution on life expectancy from China's Huai River policy. *Proceedings of*  
551 *the National Academy of Sciences* 110(32):12936-12941.
- 552 31. Central People's Government of the People's Republic of China (2017) Notice regarding the  
553 issuance of Clean Winter Heating Plan in Northern China (2017-2021).  
554 [http://www.gov.cn/xinwen/2017-12/20/content\\_5248855.htm](http://www.gov.cn/xinwen/2017-12/20/content_5248855.htm).
- 555 32. National Energy Administration (2019) Clean heating rate exceeded 5%,  
556 [https://www.sohu.com/a/362593452\\_465972](https://www.sohu.com/a/362593452_465972).
- 557 33. Shi X & Brasseur GP (2020) The Response in Air Quality to the Reduction of Chinese  
558 Economic Activities during the COVID - 19 Outbreak. *Geophys. Res. Lett.* doi:  
559 <https://doi.org/10.1029/2020GL088070>.
- 560 34. Zhang R, *et al.* (2020) NO<sub>x</sub> Emission Reduction and Recovery during COVID-19 in East  
561 China. *Atmosphere* 11(4):433.
- 562 35. Huang T, *et al.* (2017) Spatial and temporal trends in global emissions of nitrogen oxides from  
563 1960 to 2014. *Environ. Sci. Technol.* 51(14):7992-8000.
- 564 36. Huang Y, *et al.* (2014) Quantification of Global Primary Emissions of PM<sub>2.5</sub>, PM<sub>10</sub>, and TSP  
565 from Combustion and Industrial Process Sources. *Environ. Sci. Technol.* 48(23):13834-13843.
- 566 37. Shen H, *et al.* (2017) Urbanization-induced population migration has reduced ambient PM<sub>2.5</sub>  
567 concentrations in China. *Science Advances* 3(7):e1700300.
- 568 38. Shen HZ, *et al.* (2018) Impacts of rural worker migration on ambient air quality and health in  
569 China: From the perspective of upgrading residential energy consumption. *Environ. Int.*  
570 113:290-299.
- 571 39. Ministry of Environmental Protection (2013) *Exposure Factors Handbook of Chinese*  
572 *Population (Adult volume)* (China Environmental Science Press, 2013).
- 573 40. Zhao S, *et al.* (2019) A Multiphase CMAQ Version 5.0 Adjoint. *Geoscientific Model*  
574 *Development Discussions*. doi: <https://doi.org/10.5194/gmd-2019-287>.
- 575 41. AiMa Forecasts (2020) AiMa air quality forecasting system,  
576 [http://www.aimayubao.com/wryb\\_eval.php?movie=no](http://www.aimayubao.com/wryb_eval.php?movie=no).
- 577 42. Lyu B, Zhang Y, & Hu Y (2017) Improving PM<sub>2.5</sub> air quality model forecasts in China using  
578 a bias-correction framework. *Atmosphere* 8(8):147.
- 579 43. Energy Statistics Division of National Bureau of Statistics (2018) *China Energy Statistical*  
580 *Yearbook 2018* (China Statistics Press, Beijing, China).

- 581 44. US EPA Office of Research and Development (2014) CMAQv5.0.2. doi:  
582 <https://zenodo.org/record/1079898#.XotQSIhKg2w>
- 583 45. Skamarock WC, et al. (2008) A description of the advanced research WRF version 3.  
584 (National Center For Atmospheric Research Boulder Co Mesoscale and  
585 Microscale Meteorology Division).
- 586 46. National Centers for Environmental Prediction (2020) NCEP Products Inventory: Global  
587 Products, Global Forecast System (GFS) Model.  
588 <https://www.nco.ncep.noaa.gov/pmb/products/gfs/#GFS>
- 589 47. Hakami A, et al. (2007) The adjoint of CMAQ. *Environ. Sci. Technol.* 41(22):7807-7817.
- 590 48. Chen Y, et al. (2016) Transition of household cookfuels in China from 2010 to 2012. *Applied*  
591 *Energy* 184:800-809.
- 592 49. Johnson M, Lam N, Brant S, Gray C, & Pennise D (2011) Modeling indoor air pollution from  
593 cookstove emissions in developing countries using a Monte Carlo single-box model. *Atmos.*  
594 *Environ.* 45(19):3237-3243.
- 595 50. World Health Organization (2014) *WHO guidelines for indoor air quality: household fuel*  
596 *combustion – Review 3: Model for linking household energy use with indoor air quality*  
597 [https://www.who.int/airpollution/guidelines/household-fuel-combustion/Review\\_3.pdf?ua=1](https://www.who.int/airpollution/guidelines/household-fuel-combustion/Review_3.pdf?ua=1).
- 598 51. Xiang J, et al. (2019) Reducing Indoor Levels of “Outdoor PM<sub>2.5</sub>” in Urban China: Impact on  
599 Mortalities. *Environ. Sci. Technol.* 53(6):3119-3127.
- 600 52. Kirkwood TB (1979) Geometric means and measures of dispersion. *Biometrics* 35(4):908-  
601 909.
- 602 53. Endo Y (2009) Estimate of confidence intervals for geometric mean diameter and geometric  
603 standard deviation of lognormal size distribution. *Powder Technol.* 193(2):154-161.
- 604 54. Shen HZ, et al. (2013) Global Atmospheric Emissions of Polycyclic Aromatic Hydrocarbons  
605 from 1960 to 2008 and Future Predictions. *Environ. Sci. Technol.* 47(12):6415-6424.
- 606 55. Shi S, Chen C, & Zhao B (2017) Modifications of exposure to ambient particulate matter:  
607 Tackling bias in using ambient concentration as surrogate with particle infiltration factor and  
608 ambient exposure factor. *Environ. Pollut.* 220:337-347.
- 609

1 **Supplementary Figures and Tables**

2



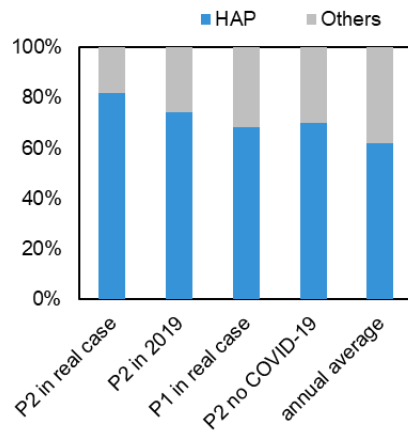
3

4 **Figure S1. HAP contributions on PWE through the direct impact on indoor air quality**  
5 **(directly to indoor), outdoor infiltration (indirectly to indoor), and the direct impact on**  
6 **outdoor air quality in China, and in urban and rural areas.**

7

8

9



10

11 **Figure S2. The contributions of HAP and other sources on national PWE during the**  
 12 **quarantine, the same period in 2019 (P2 in 2019), one month before the quarantine (P1 in**  
 13 **real case), the same period but with no COVID-19 outbreak (P2 no COVID-19), and for**  
 14 **annual average.**

15

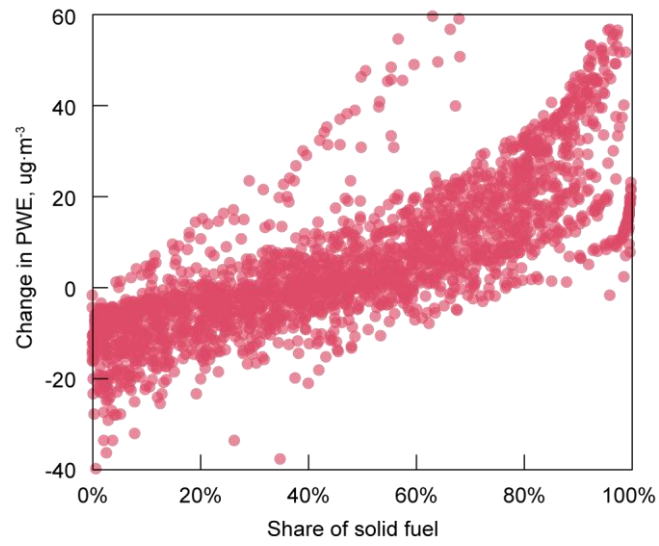
16

17

18

19





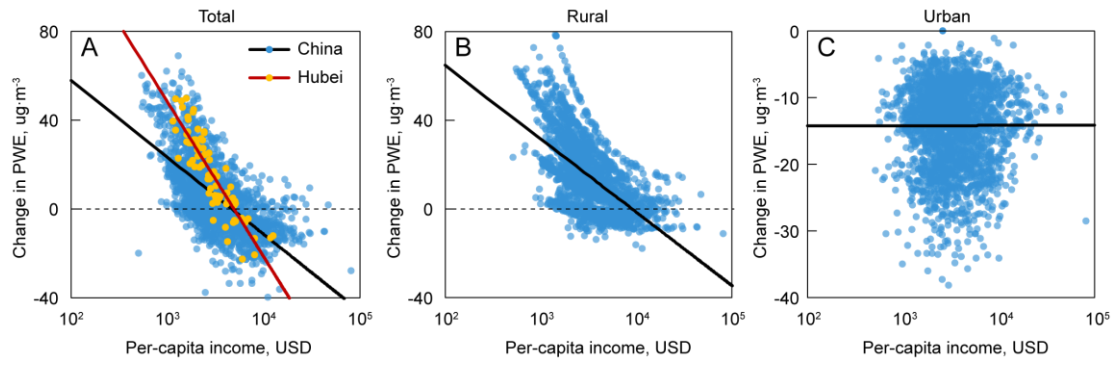
20

21 **Figure S3. The relationship between the share of solid fuel in household energy use and the**  
22 **change in PWE due to the COVID-19-induced quarantine.**

23

24

25



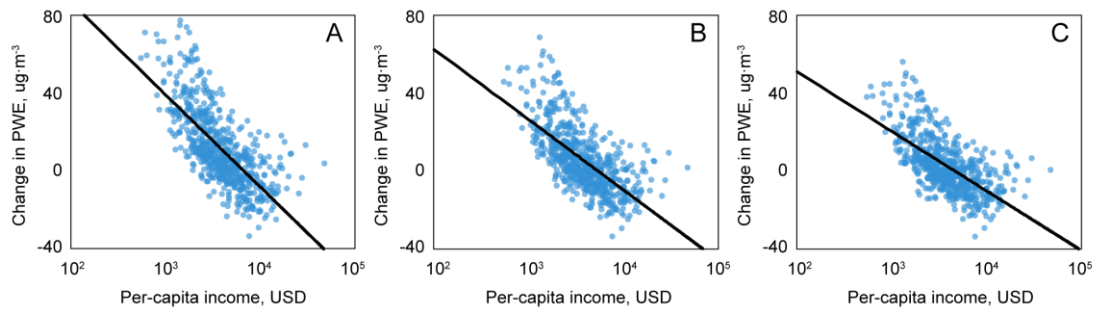
26

27 **Figure S4. The relationship between per-capita income and PWE change in China (A) and in**  
 28 **rural (B) and urban (C) areas separately. In panel A, the trend in Hubei is also illustrated.**

29

30

31



32

33 **Figure S5. The relationship between per-capita income and the quarantine-induced changes**

34 **in PWE in the heating region in the “no clean plan” case (A), the real case (B), and the “full**

35 **phase in” case (C).** In the “no clean plan” case (A), it is assumed that there was no “Clean

36 Heating Plan”, where the energy mix was mainly driven by per-capita income. In the “full phase

37 in” case (C), the “Clean Heating Plan” is assumed to be fully phased in as in 2021 which is the

38 ending year of the various targets set in the plan.

39

40

41 **Table S1. Time spent indoors by province before and during the quarantine, in hour per day.**

Province	Severity <sup>a</sup>	Before		During		
		Urban	Rural	Urban	Rural	
Anhui	4	21.3	20.5	23.2	23.0	21.3
Beijing	3	21.0	20.6	23.0	22.9	21.0
Fujian	3	21.3	20.5	23.1	22.8	21.3
Gansu	2	21.1	20.3	22.8	22.5	21.1
Guangdong	4	20.5	20.1	23.0	22.9	20.5
Guangxi	3	20.5	20.1	22.8	22.7	20.5
Guizhou	2	20.3	20.0	22.5	22.4	20.3
Hainan	2	20.5	20.1	22.6	22.4	20.5
Hebei	3	21.0	20.6	23.0	22.9	21.0
Henan	4	21.0	20.6	23.1	23.0	21.0
Heilongjiang	3	22.5	22.2	23.5	23.4	22.5
Hubei	5	20.5	20.1	23.5	23.5	20.5
Hunan	4	20.5	20.1	23.0	22.9	20.5
Jilin	2	22.5	22.2	23.4	23.3	22.5
Jiangxi	4	21.3	20.5	23.2	23.0	21.3
Jiangsu	3	21.3	20.5	23.1	22.8	21.3
Liaoning	2	22.5	22.2	23.4	23.3	22.5
Nei Mongol	2	21.0	20.6	22.8	22.6	21.0
Ningxia	2	21.1	20.3	22.8	22.5	21.1
Qinghai	1	21.1	20.3	21.9	21.3	21.1
Sichuan	3	20.3	20.0	22.8	22.7	20.3
Shaanxi	3	21.1	20.3	23.0	22.8	21.1
Shandong	3	21.3	20.5	23.1	22.8	21.3
Shanghai	3	21.3	20.5	23.1	22.8	21.3
Shanxi	2	21.0	20.6	22.8	22.6	21.0
Tianjin	2	21.0	20.6	22.8	22.6	21.0
Xinjiang	2	21.1	20.3	22.8	22.5	21.1
Tibet	1	21.1	20.3	21.9	21.3	21.1
Yunnan	2	20.3	20.0	22.5	22.4	20.3
Zhejiang	4	21.3	20.5	23.2	23.0	21.3
Chongqing	3	20.3	20.0	22.8	22.7	20.3

42 <sup>a</sup> “Severity” denotes the epidemic severity of the province, ranging from 1 (the least severe) to 5  
43 (the most severe).

44

45